INTERNATIONAL JOURNAL FOR NUMERICAL METHODS IN FLUIDS, VOL. 20, 319–334 (1995)

FINITE ELEMENT MODELLING OF THE FLOW OF CHEMICALLY REACTIVE POLYMERIC LIQUIDS

L. LEFEBVRE AND R. KEUNINGS*

Unité de Mécanique Appliquée, Université Catholique de Louvain, B-1348 Louvain-la-Neuve, Belgium

SUMMARY

We consider steady state and time-dependent flows of chemically reactive polymeric systems in two-dimensional geometries. A numerical simulation tool is proposed for predicting the evolution of the macroscopic velocity, temperature, stress and species concentration fields in such flows. We formulate a general mathematical model on the basis of the first principles of continuum mechanics, which includes a description of the non-linear coupling between kinematics, heat transfer and chemical kinetics. The resulting set of non-linear partial differential equations is solved numerically by means of appropriate finite element techniques. We have implemented the resulting numerical model in the general-purpose POLYFLOW® software developed in Louvain-la-Neuve, Belgium. Simulation results for various steady state and time-dependent reactive flows are reported.

KEY WORDS Chemically reactive flows Finite element analysis Polymeric fluids

1. INTRODUCTION

Computer modelling techniques applied to polymer processing are being developed at a fast pace.[1] In particular, simulation methods that account for the complex rheological behaviour of polymer systems have been significantly improved over the last decade.[2,3] to the extent that robust commercial software is now used in industrial developments.[4] In the present paper we wish to extend these modelling capabilities by considering chemically reactive polymeric flows.

Three main issues must be dealt with in order to describe chemically reactive flows of polymeric systems. First, one needs a proper mathematical description of the relevant chemical kinetics. Second, the effect on the fluid rheological behaviour of structure build-up due to the reactive processes must be characterized. Third, appropriate numerical algorithms are required for the solution of the set of non-linear partial differential equations describing the system. These issues arise in most processes of industrial relevance. A prime example is that of processing of polyurethane foams.[5] Indeed, processing flows of urethane foaming systems involve a material whose molecular and supramolecular structures are rapidly evolving as the chemical reactions proceed. Here, the gas phase contributing to foaming is produced together with the continuous polymeric phase. Foaming and polymerization processes are both highly exothermic. Moreover, important density variations are obtained in a matter of minutes, which has a major impact on the flow kinematics.[6] Finally, the rheological behaviour of the foaming system changes dramatically as the chemical reactions proceed.

* Author to whom correspondence should be addressed.

CCC 0271–2091/95/040319–16

Received 4 January 1994
Revised 23 July 1994

A complete micromechanical description of the above physicochemical processes that could be used for general flow simulations is not feasible with current computing resources. As a first step we have thus opted to consider the chemically reactive polymeric system under investigation as a macroscopically single-phase material. We wish, however, to predict the evolution of the different chemical species contributing to the macroscopic behaviour of the system. In order to do so, we propose a general set of governing equations derived from the first principles of continuum mechanics. To those general equations we add a number of phenomenological relations for the chemical kinetics and the evolving fluid rheology.

The numerical solution of the resulting set of governing equations for flow processes of industrial relevance requires the development of a sophisticated non-linear finite element methodology. The main issues here are the mixed mathematical nature of the governing equations, the strong non-linear coupling between kinematics, heat and mass transfer, and the possible presence of free surfaces. These difficulties are addressed in this work by means of a panoply of numerical schemes based on modern finite element techniques. We have implemented the resulting numerical model in the commercial computer code POLYFLOW^{R} that allows for the prediction of multidimensional flows in complex geometries.[4]

The paper is organized as follows. In Section 2 we propose a macroscopic mathematical formulation of chemically reactive polymeric flows. When deemed necessary, the case of polyurethane foams is used for illustrative purposes. The numerical technique is briefly described in Section 3. Since the main ingredients of our numerical approach have been published elsewhere by various authors (in the context of Navier–Stokes and chemically neutral polymer flows), we only focus on the basic features and refer to the literature for details. Simulation results are reported in Section 4. Three flow problems are considered, involving fluid systems with six different chemical species: (i) the time-dependent confined flow in a divergent die, (ii) a steady state flow in a heated die (inverse problem) and (iii) the transient, free surface, 'free-rise' flow in a cylindrical reactor.

2. MATHEMATICAL MODEL

Let us consider a chemically reactive polymeric system involving Nc simultaneous chemical reactions. We shall assume a total of Nr different reactants and Np different products. Our goal is to predict the evolution of the chemical reactions, namely the evolving volume fractions of the $Nr + Np$ species, together with that of the macroscopic velocity, stress and temperature fields. In particular, we are interested in describing the complex non-linear coupling between kinematics, heat transfer, rheology and chemical reactions.

In order to build a computationally tractable mathematical model, we consider the chemically reactive system as a compressible, purely viscous, homogeneous fluid. By compressibility we mean here that the overall fluid density is a function of temperature but not of pressure. This applies, for example, to the case of polyurethane foam processing. We shall neglect mass transfer by diffusion, and all species physical properties are assumed constant. The primary unknowns of the model are the macroscopic velocity, pressure, temperature and species volume fraction fields. In addition, free surface parameters are also part of the unknowns when the process involves free surfaces.

Our basic mathematical model then consists of (i) kinetics laws and rheological constitutive equations (both being specific to each particular reactive system under investigation), (ii) conservation equations for linear momentum, mass and energy, (iii) a kinematic equation describing the motion of free surfaces (if any) and (iv) suitable initial and boundary conditions specified for the unknown fields. Material data are needed for describing the chemical kinetics as well as the rheological and thermal behaviour of the system. Let us consider in sequence the various components of the model.

We define, for each of the $Nr + Np$ species involved, the volume fraction α_i, the rate of formation or disappearance r_i, the heat capacity c_i, the thermal conductivity k_i, and the density ρ_i. In order to predict the evolution of the volume fraction fields, we shall need suitable kinetics equations that describe the relevant chemical reactions. As an example, let us consider the case of polyurethane foam processing. Here the material evolves from a low-molecular-weight, dilute emulsion to a structured fluid in which gas bubbles are separated by thin polymeric liquid films. The gas phase is generated within the liquid phase as a by-product of the polymerization reaction. Production of the blowing agent and curing of the polymer occurs simultaneously; both processes are highly exothermic.[5] The two primary chemical reactions occurring in polyurethane foam processing involve three main reactants: a hydroxyl-group-ended resin R′-$(OH)_{f1}$ (**1**), polyisocyanate R-$(NCO)_{f2}$ (**2**) and water (**4**). Described here for monofunctional reactants (i.e. $f1 = f2 = 1$), these reactions are the so-called *gelling reaction*

$$\underset{\mathbf{1}}{\mathrm{R'-OH}} + \underset{\mathbf{2}}{\mathrm{RNCO}} \rightarrow \underset{\mathbf{3}}{\mathrm{R'-O-OC-NH-R}}, \tag{1}$$

which leads to the formation of polyurethane (**3**), and the *blowing reaction*

$$\underset{\mathbf{2}}{\mathrm{2R-NCO}} + \underset{\mathbf{4}}{\mathrm{H_2O}} \rightarrow \underset{\mathbf{5}}{\mathrm{CO_2}} + \underset{\mathbf{6}}{\mathrm{R-NH-CO-NH-R}}, \tag{2}$$

which produces the blowing agent, i.e. carbon dioxide (**5**) and polyurea (**6**). In our notation, we have here $Nc = 2$, $Nr = 3$ and $Np = 3$. We have shown[6] that second-order kinetics apply for both the gelling and blowing reactions. This means, for example, that the rate of production of urethane ($i = 3$) is given by

$$r_3 = K_A \exp(-E_A/RT)\alpha_1\alpha_2 , \tag{3}$$

where the subscripts 1 and 2 refer to isocyanate and resin respectively, R is the gas constant and T is the absolute temperature. The kinetics model (3) involves two material parameters, namely the pre-exponential factor K_A and the activation energy E_A. Similarly, the rate of production of carbon dioxide ($i = 5$) is described by

$$r_5 = K_B \exp(-E_B/RT)\alpha_2\alpha_4 , \tag{4}$$

where the subscript 4 refers to water. The two chemical reactions of our example will generate heat in the respective amounts H_A and H_B. The kinetic expressions (3) and (4) and the heats of reaction H_A and H_B will serve as source terms in the conservation equations for mass and energy respectively. In the present work all species densitiesρ_i are constant, expect that of CO_2 which follows the perfect gas law.

The accurate mathematical description of the rheology of reactive polymeric systems remains for the most part an open issue. In view of the lack of detailed theories, we suppose that we have at our disposal a phenomenological, viscous constitutive equation of the form

$$\mathbf{T} = 2\mu_f(\alpha_j , T, \dot{\gamma})\mathbf{D} , \tag{5}$$

which relates the extra-stress tensor $\mathbf{T}$ to the rate-of-strain tensor $\mathbf{D}$ through the shear viscosity μ_f; the latter is a function of the degree of advancement of the chemical reactions, of the shear rate $\dot{\gamma}$ and of temperature. We have proposed such a model in the context of polyurethane foam processing.[6,7] A general constitutive law of the form (5) has been implemented in the code. We point out, however, that in the flow processes reported in the present paper, the rheology of the system has been found to play a very minor role relative to that of the chemically induced density variations.

We can now state the governing equations using the basic principles of continuum mechanics. The momentum, energy and global mass conservation equations read respectively

$$\rho_f\left(\frac{\partial \mathbf{v}}{\partial t} + \mathbf{v}\cdot\nabla\mathbf{v}\right) = -\nabla p + \nabla\cdot\left[2\mu_f(\alpha_j,\ T,\ \dot{\gamma})\mathbf{D}\right], \tag{6}$$

$$\rho_f C_f\left(\frac{\partial T}{\partial t} + \mathbf{v}\cdot\nabla T\right) = \nabla\cdot(k_f\nabla T) + H(\alpha_j) + \mathbf{T}:\nabla\mathbf{v}, \tag{7}$$

$$\frac{\partial \rho_f}{\partial t} + \nabla\cdot(\rho_f\mathbf{v}) = 0. \tag{8}$$

In these equations, $\mathbf{v}$ stands for the velocity vector, p is the pressure, ρ_f is the fluid density, k_f is the heat conductivity, C_f is the heat capacity and H is the total heat generated by the Nc reactions. The density is given by

$$\rho_f = \sum_{i=1}^{Nr+Np}(\alpha_i\rho_i). \tag{9}$$

We approximate the heat capacity and conductivity by the relations

$$k_f = \sum_{i=1}^{Nr+Np}(\alpha_i k_i) \qquad \rho_f C_f = \sum_{i=1}^{Nr+Np}(\alpha_i\rho_i c_i)\ . \tag{10}$$

In addition to (6–8), we write a mass conservation for the ith species ($i = 1, 2, \ldots, Nr + Np - 1$) as

$$\frac{\partial(\rho_i\alpha_i)}{\partial t} + \nabla\cdot(\rho_i\alpha_i\mathbf{v}) = r_i(\alpha_j,\ T), \tag{11}$$

where r_i is the rate of formation or disappearance of the ith species, given e.g. by (3). Finally, the following algebraic constraint applies:

$$\sum_{i=1}^{Nr+Np}\alpha_i = 1\ . \tag{12}$$

Equations (6–8), (11) and (12) are used to compute steady state or time-dependent reactive flows in confined geometries. The simulation of many flows of industrial interest involves the prediction of free surfaces whose location is *a priori* unknown. A similar issue arises in the study of co-flow of immiscible fluids (e.g. in co-extrusion processes). In this latter case the interfaces separating immiscible adjacent fluid layers must also be determined as part of the solution to the governing equations. An additional kinematic equation is needed to compute the evolution of free surfaces. It reads

$$\mathbf{v}\cdot\mathbf{n} = \frac{\partial}{\partial t}\chi(\mathbf{x}_0,\ t)\cdot\mathbf{n}\ , \tag{13}$$

where $\mathbf{n}$ is the unit vector normal to the free surface, itself described by the vector equation $\mathbf{x} = \chi\ (\mathbf{x}_0,\ t)$, and $\mathbf{v}$ is the velocity field evaluated at the free surface.

Finally, the mathematical formulation is closed with suitable boundary and initial conditions specified for the unknown fields.

3. NUMERICAL TECHNIQUE

The governing equations (6)–(8) and (11)–(13) form a set of coupled, non-linear partial differential equations. The base numerical issues that arise are the mixed mathematical type of the governing equations, the convection-dominated nature of the energy and species conservation laws, the strong non-linear coupling between the various unknown fields and, possibly, the presence of free surfaces. These issues have been addressed separately by several authors over the last decade in the context of Newtonian and chemically neutral polymeric flows. In the present work our approach has been to combine the best available algorithms in order to define a robust and computationally tractable solution strategy for the governing equations at hand. Below we briefly outline the main ingredients of the numerical technique. Further details can be found in the listed references.

We solve the set of equations (6)–(8) and (11)–(13) approximately by means of a mixed finite element discretization of the primary unknown fields. After extensive numerical experimentation[7] we found it appropriate to use Galerkin's principle to discretize the momentum, volume fraction constraint and global mass conservation equations. On the other hand, we have implemented the consistent streamline upwind Petrov–Galerkin method (SUPG) developed by Brooks and Hughes[8] for solving the convection-dominated energy and species conservation equations. SUPG has been used with success in other hyperbolic problems, e.g. for the discretization of differential viscoelastic constitutive equations.[9]

Free surfaces are computed together with the other unknown fields by means of the technique of 'spines' advanced by Kistler and Scriven[10] for Newtonian flows and further developed in the context of polymer flows by several authors.[11–13] Here Galerkin's principle is adopted for the discretization of the kinematic condition (13).

The selection of approximation subspaces is not a trivial issue, since no rigorous mathematical analysis is available for the governing equations (6)–(8) and (11)–(13). Numerical experiments[7] with various mixed finite element interpolations for the unknown fields have guided us to the following selection: P^1-C^0 shape functions for pressure, temperature and species volume fractions; P^2-C^0 shape functions for velocity and free surface parameters. Clearly this leads to a large number of nodal unknowns even for two-dimensional problems.

In the case of steady state flows we obtain a set of non-linear algegraic equations for the nodal values of the unknown fields. We solve this set of equations by means of a full Newton scheme for the case of confined flows. A decoupled technique[11,12] is used to solve free surface flows, whereby the conservation equations are solved on a given domain by means of Newton's method at each iteration on the free surface. Finally, an automatic continuation procedure[4] on material properties and boundary conditions is used to guide the non-linear iterations.

In the case of time-dependent flows the discretized finite element equations form a set of first-order, non-linear, coupled differential equations. We discretize those equations in time by means of a first-order predictor–corrector scheme proposed by Gresho *et al.*[14] for the Navier–Stokes equations. The time step is automatically evaluated by the algorithm in order to keep the local time discretization errors within user-defined bounds. Here again a decoupled scheme is used in the case of free surface flows.[7]

4. SIMULATION RESULTS

We consider three flow problems: (I) the time-dependent confined flow in a divergent die, (II) a steady state flow in a heated die (inverse problem) and (III) the transient, free surface, 'free rise' flow in a cylindrical reactor. The first two flows are planar, while the third is axisymmetric. In all cases there are

two simultaneous chemical reactions involving six different species:

$$\begin{aligned} &\textit{reaction A}: \quad \text{reactant 1} + \text{reactant 2} \rightarrow \text{product 3}, \\ &\textit{reaction B}: \quad \text{reactant 2} + \text{reactant 4} \rightarrow \text{product 5} + \text{product 6}. \end{aligned} \tag{14}$$

We have here $Nc = 2$, $Nr = 3$ and $Np = 3$. Second-order kinetics are assumed to hold for the two reactions, as in (3) and (4). The particular material and geometrical data selected for the simulations are listed elsewhere.[7] Note that in all reported results we assume that the viscosity of the fluid is constant. Simulations with non-linear viscosities, as in (5), have shown that the rheology plays a negligible role in the three problems under investigation in comparison with the chemically induced density variations.[7] The computations were run on CRAY Y-MP and CONVEX C240 vector computers (one processor). Typical CPU times are of the order of 1 h.

4.1 Flow in a divergent die

The flow geometry consists of a smooth, two-dimensional divergent die whose walls are thermally insulated (Figure 1). The fluid is a water-blown polyurethane foam. It enters the flow domain at room tempeature with a uniform longitudinal velocity. We specify that the chemical reactions (1) and (2) start at the inlet section with prescribed reactant volume fractions. The fluid is assumed to slip at the divergent walls.* Finally, fully developed conditions are specified at the outlet section. In the present simulation the blowing agent (CO_2) density was artificially increased by a factor of 10 in order that most of the blowing reaction occur in the diverging zone of the flow domain.

Figure 2 shows the two finite element meshes used for the simulations. The coarse mesh involves 2306 unknown nodal variables, while the refined mesh contains 4618 variables. Since there is no reference solution available in the literature, a mesh refinement analysis is necessary to assess the numerical accuracy of our results. We shall see that the coarse mesh already provides accurate results.

Two cases were considered: (i) the simulation of steady state reacting flow with the inlet reactant volume fractions specified as in Figure 1, and (ii) the time-dependent response of the reacting flow following a progressive change of those inlet conditions.

The steady state simulation has been described in detail elsewhere.[7] We found that the computed flow trajectories, which are everywhere tangent to the velocity vector field, very much resemble those obtained when the chemical reactions are turned off, namely when the fluid density is forced to remain constant. The *magnitude* of the velocity vectors, however, is dramatically altered by the chemical processes. This can be observed in Figure 3, where we compare contour lines of the longitudinal velocity component obtained with a constant density model (which for a foam essentially is an inertialess, Stokes flow solution) and the chemically reacting system.

For the constant density fluid the velocity decreases continuously in view of the gradual increase in the flow geometry cross-section. The reactive fluid behaves very differently. The velocity *increases* in the divergent section up to a value about four times larger than the inlet velocity. This is due to the rapid decrease in fluid density related to the production of carbon dioxide (see Figure 8). Since the mass flow rate is conserved, the fluid must accelerate.

The above results reveal the important non-linear coupling between the conservation equations. They also point to a primary numerical difficulty, namely the selection of appropriate initial guesses for starting the iterative procedure. In the present work we use the Stokes solution to start the iterations. Since the Stokes solution is structurally very different from the final result, a careful continuation procedure is needed to obtain convergence of the iterative scheme.[7]

* We have actually implemented a *Navier* slip law, of which the slip condition used here is one limit case. Simulation results using the Navier condition are reported elsewhere.[7]

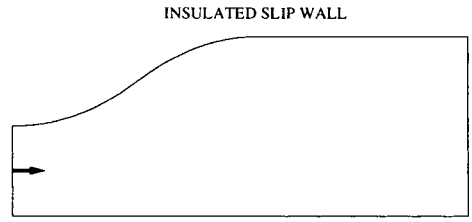

Figure 1. Computational domain. At the inlet section, we specify a uniform flow profile, a temperature of 294 K, and species volume fractions (64% resin, 32% isocyanate, 4% water). Fully developed flow is specified at the outlet section.

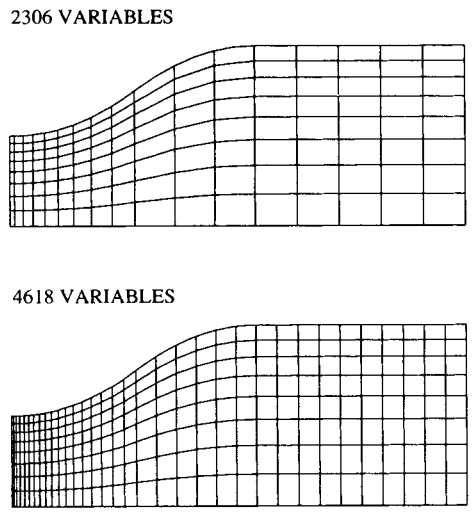

Figure 2. Finite element discretizations: coarse and refined meshes.

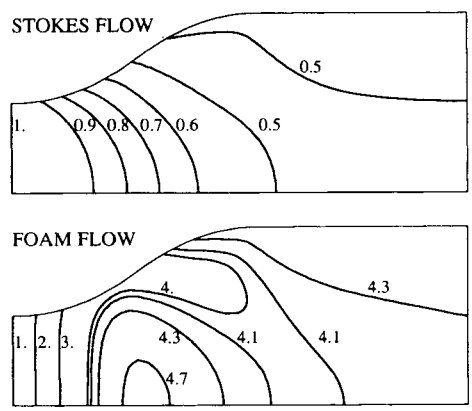

Figure 3. Normalized longitudinal velocity contours. Stokes flow: without chemical reactions; Foam flow: with chemical reactions.

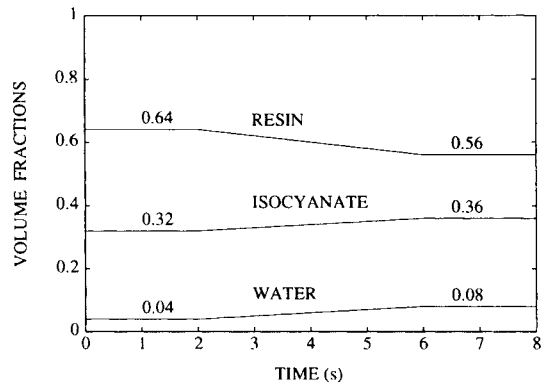

Figure 4. Time-dependent inlet conditions in terms of reactant volume fractions.

We now consider a time-dependent perturbation of the inlet boundary conditions, depicted in Figure 4. In a matter of 6s the inlet volume fractions of isocyanate and water are increased, while that of the resin is decreased. The initial conditions are given by the steady state solution described above. During the first 2s the inlet conditions are kept constant; this allows us to initiate the time integration procedure with two large time steps. After 6s the inlet conditions have reached a new steady state regime. We wish to compute the time-dependent response of the reacting flow following the change in reactant volume fractions; this change may or may not lead eventually to a new steady state regime.

In order to examine the computed results, we consider various predicted fields along the specific flow line shown in Figure 5. This flow line is a particle trajectory computed for the initial steady state flow. It is not, of course, a particle trajectory for the transient phase (nor is it one for the final steady state, if any).

Figure 6 shows the temporal evolution of the volume fraction of urethane along the curve of Figure 5. As mentioned above, the time step is computed automatically by the algorithm; its minimum value is 0·05s. The full curves have been obtained with the refined mesh, while the data points correspond to the coarse discretization (Figure 2). Agreement between the two finite element discretizations is rather good.

We find that steep gradients in species volume fractions develop during the transient phase, until a new steady state regime is reached after about 30s.

Similarly, we plot in Figure 7 the evolution of temperature along the selected curve. The exothermic character of the two chemical reactions leads to a significant spatial rise of the steady state temperature fields. The transient phase is quite complex; the temperature field *decreases* over part of the flow domain at early times.

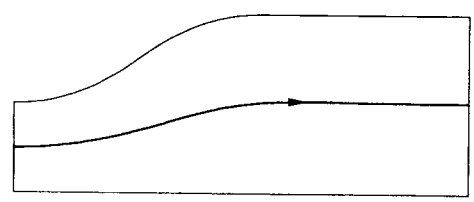

Figure 5. Flow trajectory of the initial steady-state solution selected for display of computed fields.

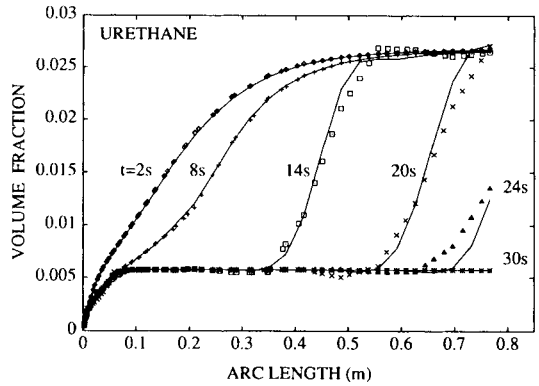

Figure 6. Computed urethane volume fraction along the curve defined in Figure 5. Coarse mesh (dots) and refined mesh (continuous lines) results, at selected values of time.

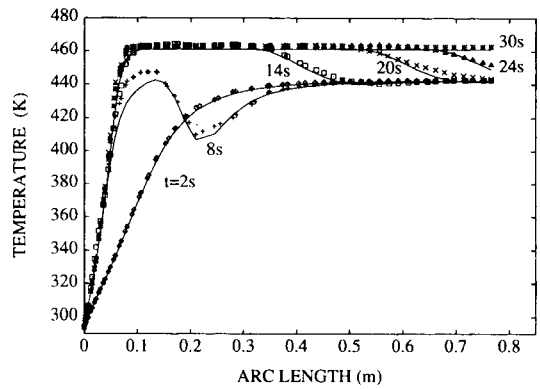

Figure 7. Computed temperature along the curve defined in Figure 5. Coarse mesh (dots) and refined mesh (continuous lines) results, at selected values of time.

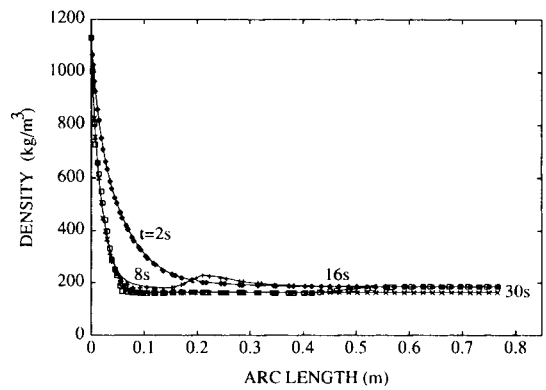

Figure 8. Computed density along the curve defined in Figure 5. Coarse mesh (dots) and refined mesh (continuous lines) results, at selected values of time.

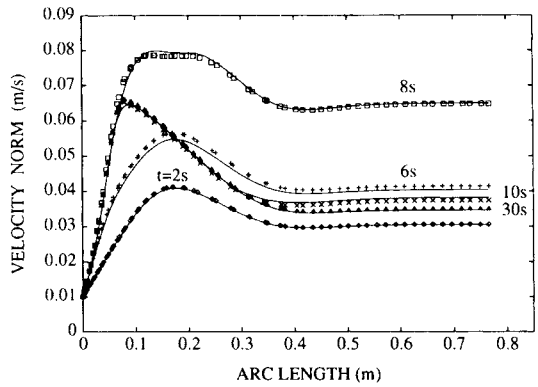

Figure 9. Computed magnitude of the velocity field along the curve defined in Figure 5. Coarse mesh (dots) and refined mesh (continuous lines) results, at selected values of time.

Figure 8 shows the predicted foam density. In the present problem, the difference between the initial and final steady state values is not large. The significant spatial decrease in density has, however, a strong impact on the flow kinematics. This can be seen in Figure 9, where we show the magnitude of the velocity vector along the selected curve. Although the final steady state velocity is not dramatically different from the initial regime, the transient phase shows a significant overshoot which has been confirmed by mesh refinement. It is clear that these complex phenomena can only be predicted by means of a non-linear simulation tool.

4.2. Steady state flow in a heated die (inverse problem)

The physical process under consideration is shown in Figure 10. The computational domain is divided into three parts: a heater, a solid die and the chemically reactive fluid. The fluid enters on the left with a specified temperature and a flat velocity profile. Is is assumed to slip at the die wall, and fully developed conditions are imposed at the exit section. We formulate the following *inverse* problem: how much heat must be generated by the heater in order to achieve a temperature of 300 K at some specified location within the flow domain? The Lagrange multiplier technique recently developed by Legat and Marchal[15] is used here to solve the inverse problem, in conjunction with the numerical method of Section 3.

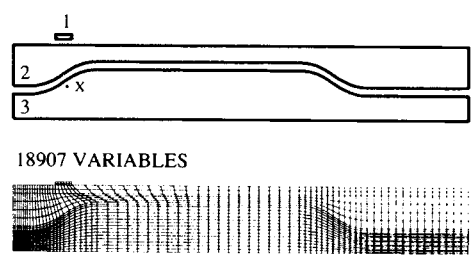

Figure 10. Exploded view of the computational domain and refined finite element discretization. Domain 1: heater; Domain 2: die; Domain 3: fluid. The temperature must reach a specified value at point X.

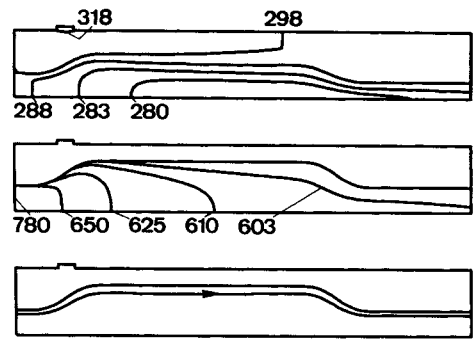

Figure 11. (top) Temperature contours (K); (middle) Fluid density contours (kg/m3); (bottom) Flow trajectory selected for display in subsequent figures.

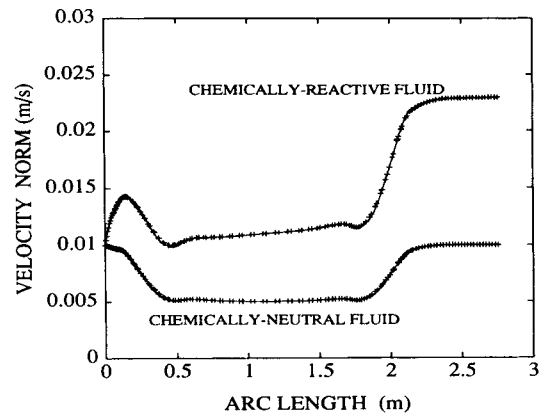

Figure 12. Norm of velocity vector (m/s) along trajectory shown in figure 11 (bottom). Coarse mesh (dots) and refined mesh (continuous lines) results. Also shown are the results obtained for the equivalent, chemically neutral fluid.

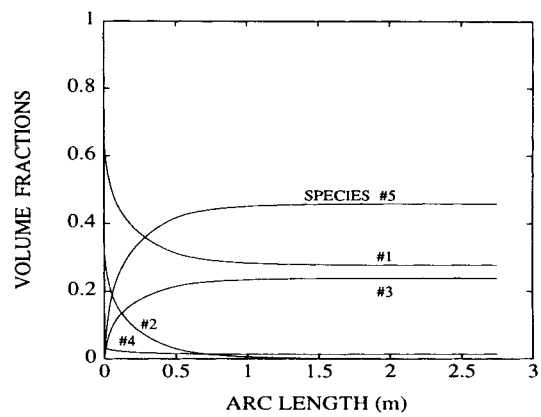

Figure 13. Evolution of species volume fractions along trajectory shown in Figure 11 (bottom).

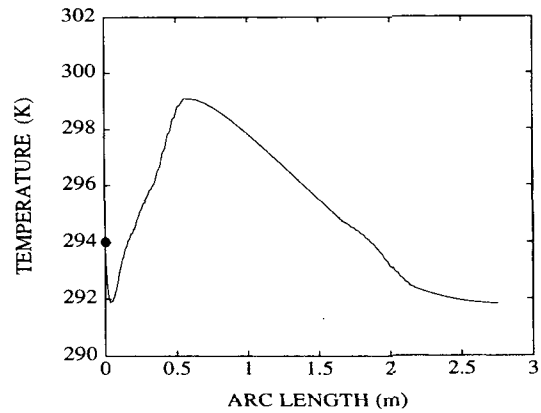

Figure 14. Evolution of temperature (K) along trajectory shown in figure 11 (bottom).

The flow involves the two chemical reactions shown in (14). One assumes that reaction A is exothermic and reaction B is endothermic. Vanishing values for the volume fractions of products are specified at the entry section, while non-stoichiometric values are imposed for the reactants. Conditions of perfect thermal insulation are imposed at the outer boundary of the 'heater' and 'die' computational domains. We solve the heat conduction equations in those two subdomains (with an *a priori* unknown, uniform heat source in the heater), together with the governing equations of Section 2 in the fluid phase. Continuity of temperature and heat flux is obtained automatically in the finite element sense at the interface between the subdomains.

We have used two finite element meshes to discretize the computational domain. The refined mesh is shown in Figure 10; it involves a total of 18,907 unknown nodal values. The coarse mesh has 4867 nodal values. There is good agreement between the results obtained with these two meshes.

Figure 11 shows the computed temperature and fluid density contours. In this example the chemical reactions lead to a decrease in the overall density. A particular fluid trajectory is selected to display various results (Figure 11, bottom). The magnitude of the velocity vector along that trajectory is shown in Figure 12, together with the results obtained under the same conditions but without chemical reactions. As in Section 4.1, there is a marked difference between the two cases, which is due to the coupling between kinematics and chemically induced density variations.

Volume fractions predicted along the selected trajectory are shown in Figure 13. In view of the non-stoichiometric data specified at the inlet section, reactant 1 is not totally consumed when the reactions are completed.

Finally, we show in Figure 14 the computed temperature along the selected trajectory. One observes four main regimes: first, a rapid decrease due to the dominating endothermic character of reaction B; this is followed by an increase in temperature caused by heat conduction from the heater; sufficiently far away from the heater the endothermic character of reaction B prevails again; finally, when the chemical reactions are completed, the temperature reaches a constant value.

4.3. Simulation of the free rise foaming experiment

The free rise foaming process is often used to study the kinetics of particular polyurethane foam formulations. A schematic diagram of the process is shown in Figure 15. The reactants are premixed rapidly and introduced at the bottom of a thermally insulated, cylindrical reactor. Foaming is then allowed to occur freely. Production of carbon dioxide leads to a continuous decrease in density and

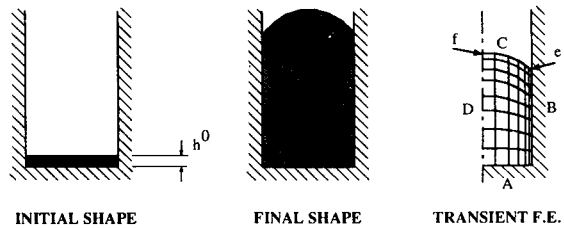

Figure 15. Schematic of free rise foaming and time-dependent computational mesh.

thus to an increase in the foam height. The reactor temperature rises owing to the exothermic nature of the chemical reactions.

We have reported previously the results of an experimental investigation of the free rise foaming process.[6] Our goal was to obtain temperature and foam height evolution profiles in order to characterize and quantify the chemical kinetics. We also developed[6] a one-dimensional mathematical model that allows for the prediction of temperature, foam height and species volume fractions as a function of time. This simplified model assumes that the process is perfectly adiabatic and that the flow is driven by density changes only. The foam flow front is thus perfectly flat in this model and dynamical forces are neglected altogether. The one-dimensional model was used to obtain the kinetic parameters on the basis of the available temperature and foam height experimental data.

In the present paper we wish to simulate the free rise foaming process by means of the two-dimensional finite element technique of Section 3, without the approximations inherent to the one-dimensional model. The flow problem is two-dimensional axisymmetric, time-dependent and involves a free surface (i.e. the foam flow front). Figure 15 shows a schematic diagram of the time-dependent computational domain and finite element discretization. The boundary of the computational domain consists of four parts. Conditions of perfect thermal insulation are imposed along the whole boundary. The foam velocity vanishes at the bottom of the reactor (side A). Side D is an axis of symmetry. Free surface boundary conditions are specified along side C. Values of the contact angle are imposed at the free surface end-points 'e' and 'f'. Finally, the foam is assumed to slip (either perfectly or partially) along the vertical reactor wall (side B). The moving finite element mesh has a total of 573 unknown nodal values. The simulation required a total of about 8000 non-linear iterations.

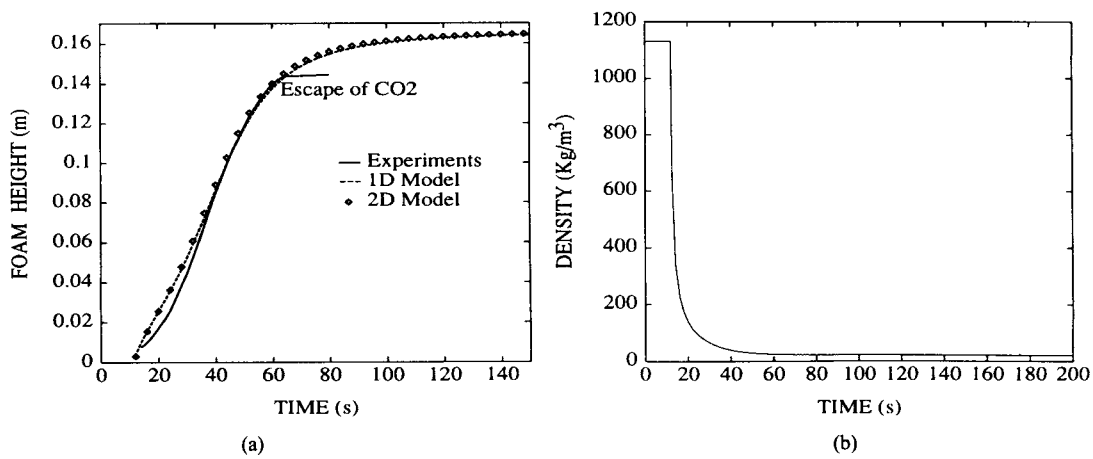

Figure 16. (a) Foam height as a function of time. Experimental observations[6] and numerical predictions obtained with the one-dimensional model[6] and the two-dimensional finite element technique (perfect slip at vertical wall); (b) computed foam density as a function of time.

As far as initial conditions are concerned, we specify homogeneous values for the reactant volume fractions as well as room temperature over the initially flat computational domain. We should point out, in relation to the experimental process, that the simulation only starts once the so-called *cream time* has been reached, namely after 12s for the particular chemical formulation considered in our work. As the simulation proceeds, the foam flow front moves vertically owing to production of the blowing agent; this is accompanied by a continuous deformation of the finite element mesh.

Two cases were studied: (i) perfect slip conditions at the vertical reactor wall (the free surface thus remains flat) and (ii) partial slip described by a Navier condition.

When perfect slip occurs at the vertical wall, the mathematical problem is exactly described by the one-dimensional model.[6] This provides a non-trivial test problem for our two-dimensional finite element procedure. We compare in Figure 16(a) the predicted time-dependent foam height obtained by means of the one-dimensional model and the two-dimensional finite element method. Agreement is excellent. Also shown in Figure 16(a) are the experimental observations.[6] The predictions are in good agreement with the experimental data, until the blowing agent is observed to escape from the top of the foam after 1 min or so. This event can obviously not be predicted with the present mathematical model.

The predicted foam density is shown in Figure 16(b). The significant decrease in density is due to the production of carbon dioxide; it is of course directly related to the foam height increase depicted in Figure 16(a).

Results obtained with partial slip at the vertical wall are discussed next. Figure 17 shows successive foam flow fronts as well as the initial and final (steady state) finite element meshes. In the present case the free surface is no longer flat in view of the viscous forces acting near the wall. Except in a small zone near the moving contact point 'e' (see Figure 15), we find that the computed temperature and volume fraction fields remain essentially homogeneous in space.

The evolution of temperature is shown in Figure 18(a). We observe that the steady state is not yet reached after 200s, even though the final foam height is attained after 120s. This is due to the vastly different kinetics of the blowing and gelling reactions, as inspection of Figure 18(b) further reveals. Here we show the predicted water and polyurethane volume fractions as a function of time. While most of the water has disappeared after 120s owing to the blowing reaction, the gelling reaction continues to produce polyurethane after 200s.

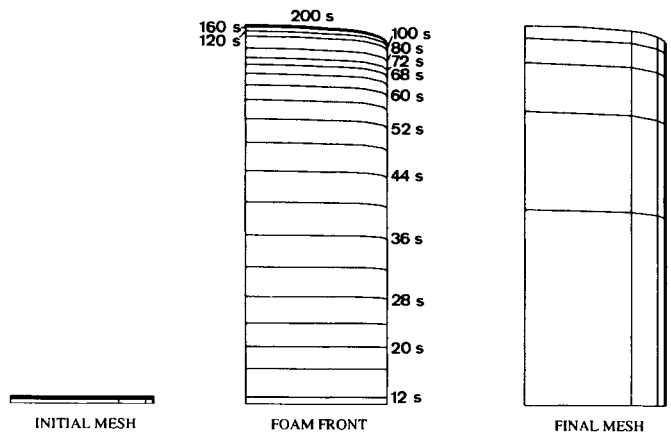

Figure 17. Evolution of foam flow front as a function of time; initial and final steady-state finite element meshes (partial slip at vertical wall).

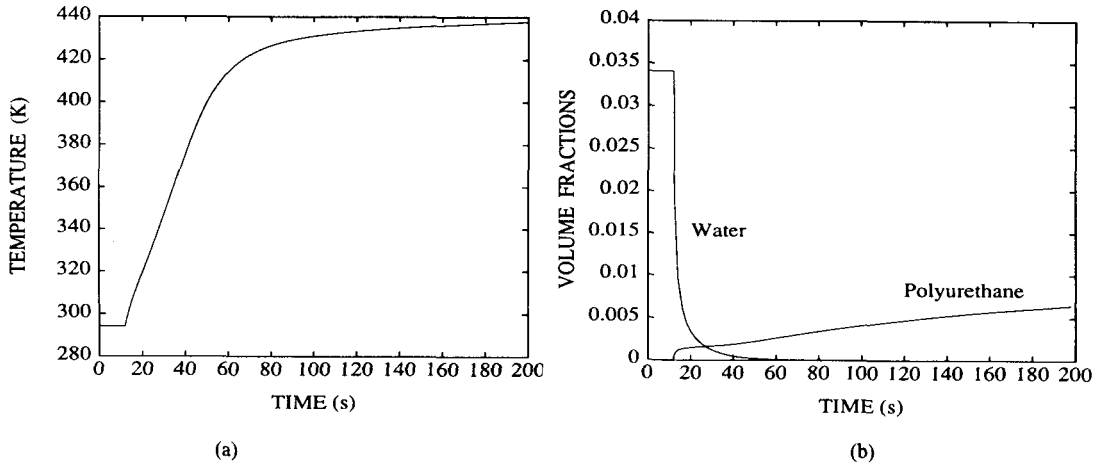

Figure 18. Computed foam temperature (a) and volume fractions of water and polyurethane (b) as a function of time.

5. CONCLUSIONS

We have described a macroscopic approach to the mathematical modelling of chemically reactive polymeric fluids. A variety of specialized finite-element-based algorithms developed for chemically neutral processing flows has been exploited to solve the resulting non-linear governing equations. Simulations have been carried out for various flow problems. The results reveal the dramatic influence on flow kinematics of the chemically induced density variations. Implementation of the proposed numerical model in a general-purpose software provides a new simulation tool that can be used fruitfully for the design of chemically reactive flow processes in the polymer industry.

This work is obviously a first step. From the computational viewpoint, extension to three-dimensional flow processes is not feasible on classical, sequential computers, and exploitation of parallel finite element algorithms is required. The work of our team in that direction is reviewed elsewhere.[16] As far as modelling is concerned, a major challenge is the development of a 'micro–macro' mathematical formulation that, on one hand, would relate the evolving microstructure of the chemically reactive polymeric systems to their macroscopic behaviour and, on the other hand, would remain computationally tractable for general flow simulations.

ACKNOWLEDGEMENTS

The doctoral work of L. Lefebvre has been supported financially by a grant from Shell Research Louvain-la-Neuve, Belgium. This text presents research results obtained in the framework of the Belgian Programme on Interuniversity Poles of Attraction initiated by the Belgian State, Prime Minister's Office for Science, Technology and Culture. The scientific responsibility is assumed by its authors.

REFERENCES

1. C. L. Tucker III (ed.), *Fundamentals of Computer Modelling for Polymer Processing*, Carl Hanser, Munich, (1989).
2. M. J. Crochet, 'Numerical simulation of viscoelastic flow: a review', *Rubber Chem. Technol.*, **62**, 426–455 (1989).
3. R. Keunings, 'Simulation of viscoelastic fluid flow', in C. L. Tucker III (ed.), *Fundamentals of Computer Modelling for Polymer Processing*, Carl Hanser, Munich, 1989, pp. 402–470.

4. M. J. Crochet, B. Debbaut, R. Keunings and J. M. Marchal, 'Polyflow: a multi-purpose finite element program for continuous polymer flows', in K. T. O'Brien (ed.), *Computer Modelling for Extrusion and Other Continuous Polymer Processes*, Carl Hanser, Munich, 1992, 25–50.
5. G. Oertel (ed.), *Polyurethane Handbook*, Carl Hanser, Munich, 1985.
6. L. Lefebvre and R. Keunings, 'Mathematical modelling and computer simulation of the flow of chemically-reacting polymeric foams', in M. Cross, J. F. T. Pittman and R. D. Wood (eds), *Mathematical Modelling for Materials Processing*, Clarendon, Oxford, 1993, pp. 399–417.
7. L. Lefebvre, *Ph.D. Thesis*, Université Catholique de Louvain, 1993.
8. A. N. Brooks and T. J. R. Hughes, 'Streamline upwind/Petrov–Galerkin formulations for convection dominated flows with particular emphasis on the incompressible Navier–Stokes equations', *Comput. Methods Appl. Mech. Eng.*, **32**, 199–259 (1982).
9. M. J. Crochet and V. Legat, 'The consistent streamline-upwind/Petrov–Galerkin method for viscoelastic flow revisited', *J. Non-Newtonian Fluid Mech.*, **42**, 283–299 (1992).
10. S. F. Kistler and L. E. Scriven, 'Coating flows', in J. R. A. Pearson and S. M. Richardson (eds), *Computational Anaysis of Polymer Processing*, Applied Science Publishers, London, 1983, pp. 243–299.
11. R. Keunings, 'An algorithm for the simulation of transient viscoelastic flows with free surfaces', *J. Comput. Phys.*, **62**, 199–220 (1986).
12. R. Keunings and R. Shipman, 'Finite element methods for transient viscoelastic free surface flows', in K. Mattiasson *et al.*, (eds), *Proc. 2nd Int. Conf. on Numerical Methods in Industrial Forming Processes*, Göteborg, 1986, 293–298.
13. V. Legat, *Ph.D. Thesis*, Université Catholique de Louvain, 1992.
14. P. M. Gresho, R. L. Lee and R. L. Sani, 'On the time-dependent solution of the incompressible Navier–Stokes equations in two and three dimensions', in *Recent Advances in Numerical Methods in Fluids*, Vol. 1, Pineridge, Swansea, 1980, pp.
15. V. Legat and J. M. Marchal, 'Die design: an implicit formulation for the inverse problem', *Int. j. numer. methods fluids*, **16**, 29–42 (1993).
16. R. Keunings, 'Parallel finite element algorithms applied to computational rheology', *Comput. Chem. Eng.*, in press.